

# Synthesis, Structure, and Reactions of Stable Oxametallacycles from Styrene Oxide on Ag(111)<sup>†</sup>

M. Enever,<sup>‡</sup> S. Linic,<sup>‡,§</sup> K. Uffalussy,<sup>||</sup> J. M. Vohs,<sup>#</sup> and M. A. Barteau<sup>\*†</sup>

Center for Catalytic Science and Technology, Department of Chemical Engineering, University of Delaware, Newark, Delaware 19716, Department of Chemical Engineering, University of Michigan, Ann Arbor, Michigan 48109, Department of Chemical Engineering, North Carolina State University, Raleigh, North Carolina 27685, and Department of Chemical and Biomolecular Engineering, University of Pennsylvania, Philadelphia, Pennsylvania 19104

Received: March 9, 2004; In Final Form: June 5, 2004

Styrene oxide undergoes an activated ring opening on Ag(111) at temperatures above 200 K. The product of this reaction is a stable oxametallacycle intermediate. The structure of this species has been obtained by density functional theory calculations and the computed vibrational spectrum is consistent with the experimental spectrum obtained using high-resolution electron energy loss spectroscopy. The oxametallacycle formed by ring-opening styrene oxide is structurally analogous to that previously observed for ring opening of epoxybutene on Ag(110) and represents the largest member of this adsorbate structure class yet isolated. In both cases, the epoxide ring opens at the carbon bearing the pendant unsaturated group, and the pendant group (phenyl in styrene oxide) is oriented nearly parallel to the surface plane. The oxametallacycle formed from styrene oxide reacts at 485 K to regenerate styrene oxide plus small amounts of phenylacetaldehyde. This peak temperature is similar to that previously reported for generation of styrene oxide from adsorbed styrene and oxygen atoms on Ag(111), suggesting that the epoxidation proceeds via the oxametallacycle intermediate isolated in the present work.

## Introduction

The epoxidation of olefins is an extremely important class of catalytic chemical reactions. In 1998, the domestic production of ethylene oxide (EO) was 8.14 billion lbs,<sup>1</sup> making it one of the largest volume chemicals produced by the chemical industry. Over the past two decades, considerable effort has been devoted to understanding the mechanisms of silver-catalyzed olefin epoxidation.<sup>2,3</sup> Recent curiosity has been fueled in part by the commercialization of a process for epoxidation of 1,3-butadiene to form 3,4-epoxy-1-butene (EpB).<sup>4</sup> Both the ethylene and butadiene epoxidation processes employ silver catalysts supported on  $\alpha$ -Al<sub>2</sub>O<sub>3</sub> and promoted by alkalis and halides. In addition to ethylene and 1,3-butadiene, there have been reports of the steady-state selective epoxidation of higher nonallylic olefins such as styrene<sup>5</sup> and 3,3-dimethyl-1-butene<sup>6</sup> using alumina-supported silver catalysts. Results for the epoxidation of styrene<sup>5</sup> show that such catalysts are both active and selective for the formation of styrene oxide, corroborating earlier findings of Hawker et al.<sup>7</sup> which demonstrated the formation of styrene oxide in the course of the temperature-programmed reaction of styrene on oxygen-covered Ag(111).

Mechanistic issues most often addressed have been the roles of oxygen and of promoters in these reactions. It is typically reported that atomic, rather than molecular, adsorbed oxygen reacts with ethylene,<sup>8</sup> styrene,<sup>7</sup> norbornene,<sup>9</sup> and 3,3-dimethyl-

butene<sup>10</sup> in the rate-determining step. As recently noted for ethylene and butadiene epoxidation, the oxygen dissociation rate may also be kinetically significant, even rate-controlling under some conditions.<sup>11–15</sup> However, because selectivity is likely controlled by steps occurring after the rate-determining oxygen dissociation and oxygen addition steps,<sup>14,15</sup> little progress had been made until recently in determining the nature of the organic intermediates formed during these epoxidation reactions.

There is a growing body of evidence for surface oxametallacycles as the pivotal species in selective olefin epoxidation. Stable oxametallacycles have been synthesized from 2-iodoethanol on Ag(110)<sup>16</sup> and (111)<sup>17,18</sup> surfaces, from ethylene oxide on Ag(111),<sup>19</sup> and from epoxybutene on Ag(110)<sup>20</sup> and (111). Those formed on clean silver surfaces by activated ring opening of epoxides react by ring closure to reform the parent epoxides plus small amounts of isomeric or decomposition products. Most importantly, we have been able to establish spectroscopic, kinetics, and selectivity connections for oxametallacycles to the performance of working catalysts. For example, once the characteristic vibrations of oxametallacycles were identified from HREELS and DFT studies on single crystals,<sup>19</sup> it was possible to find spectroscopic evidence for these species in the earlier IR spectra obtained by Force and Bell<sup>21</sup> for silver catalysts carrying out steady-state ethylene epoxidation. Most recently, we have shown that a microkinetic model based on oxametallacycle species can explain the activity of silver catalysts for ethylene epoxidation and that selectivity is controlled (and can be explained quantitatively) by competing reactions of the oxametallacycle to form ethylene oxide or acetaldehyde.<sup>11,15</sup> The comprehensive microkinetic model produced by Stegelmann et al.<sup>14</sup> strongly reaffirms these conclusions and supports the earlier proposals of Cant and Hall<sup>22</sup> and

<sup>†</sup> Part of the special issue "Michel Boudart Festschrift".

\* Corresponding author. Tel: 1-302-831-8905; fax: 1-302-831-8201; e-mail: barteau@che.udel.edu.

<sup>‡</sup> University of Delaware.

<sup>§</sup> University of Michigan.

<sup>||</sup> North Carolina State University.

<sup>#</sup> University of Pennsylvania.

Campbell<sup>23</sup> that the selective and nonselective channels in ethylene epoxidation involve a common intermediate. We have recently demonstrated the design of an improved bimetallic catalyst for ethylene epoxidation based on control of the oxametallacycle branching selectivity.<sup>24</sup>

As a part of continuing effort to understand the mechanism of olefin epoxidation and particularly the role that surface oxametallacycles play, we have focused on these intermediates on silver surfaces. In this work, we report results for the reaction and adsorption of styrene oxide (StO) at various temperatures on Ag(111). By analogy with previous observations for ethylene oxide and epoxybutene, it is anticipated that the ring opening of styrene oxide would be activated, leading to the formation of a stable surface oxametallacycle. In this investigation, we bring to bear spectroscopic techniques such as temperature-programmed desorption (TPD) and high-resolution electron energy loss spectroscopy (HREELS), along with density functional theory (DFT)-based calculations.

The motivation for this work stems from the fact that the proposed mechanisms of olefin epoxidation processes appear to be very similar for different olefins. To better understand the role that oxametallacycles might play, investigation of different oxametallacycles is needed. Moreover, it is expected that the styrene oxide oxametallacycle, if formed, would be stabilized on Ag by the interaction of the benzene ring  $\pi$ -electrons with the silver surface. We have previously noted that vinyl-surface interactions in EpB-derived oxametallacycles stabilize these species by about 10 kcal/mol.<sup>20</sup> Another reason that makes styrene oxide oxametallacycles very appealing is that the low reactivity of benzene ring ensures that the chemical reaction will take place at the epoxide function, resulting in a limited number of possible isomeric reaction products in TPD experiments, mainly styrene oxide, acetophenone, and phenylacetaldehyde. Also, since the creation of styrene oxametallacycles from styrene oxide requires C–O bond scission, it is interesting to determine which of the two inequivalent C–O bonds of the epoxide will be broken, the one next to the benzene ring or the one farther away from the benzene ring.

We report here isolation of a surface intermediate during the reaction of styrene oxide on Ag(111). This intermediate reacts to reform styrene oxide as a major product along with phenylacetaldehyde. Experimental and theoretical vibrational spectra identify this species as an oxametallacycle, as demonstrated below.

## Experimental Section

Experiments were performed in two UHV chambers. Temperature-programmed desorption (TPD) experiments were carried out in a chamber described previously.<sup>25</sup> The system was evacuated to the base pressure of  $1 \times 10^{-10}$  Torr. The chamber was equipped with a four-grid optics for LEED and AES experiments, a UTI 100C quadrupole mass spectrometer for TPD experiments, and a sputter ion gun for sample cleaning. The details of those TPD experiments have been described elsewhere.<sup>26</sup>

HREELS experiments were performed in a second chamber. The Ag(111) sample was mounted on a tantalum foil backing plate which was spot-welded to two tantalum foil strips placed on the sample mounting rods extending from a thermocouple feed-through. The chamber base pressure achieved was  $(1\text{--}2) \times 10^{-10}$  Torr for all experiments. The system was equipped with an LK Technologies ELS 300 spectrometer and has been described previously.<sup>27</sup> Both on-specular and off-specular spectra were collected. On-specular scans were collected with the

electron beam incident at  $60^\circ$  with respect to the surface normal. The electron beam energy was 3 eV with a full width at half-maximum (fwhm) resolution of 4.5–6 meV for the elastically scattered beam. Off-specular scans were obtained with the electron beam incident at  $65^\circ$  with respect to the surface normal. A resolution of 4.5 meV was obtained for the elastically scattered beam, and the beam energy was increased to 4 eV to enhance impact scattering effects. The system was also equipped with LEED and AES capabilities.

The silver single crystal was aligned to the (111) orientation by the Laue method, cut, and polished using standard metallographic techniques. The initial cleaning of the Ag(111) crystal was accomplished by cycles of argon ion bombardment followed by annealing to 750 K. The surface orientation and cleanliness were verified using LEED and HREELS, respectively. In both systems, sample heating was accomplished by passing a current through the tantalum wires. The styrene oxide used in the experiments (98% purity, Sigma-Aldrich) was transferred to the chamber from a glass-dosing tube through a short, stainless steel line. Styrene oxide was purified by repeated freeze–pump–thaw cycles.

## Computational Details

The Amsterdam Density Functional (ADF)<sup>28–30</sup> program, version 2002.03 was used for total energy calculations, geometry optimizations, and vibrational frequency calculations in this work. ADF is used to solve one-electron Kohn–Sham equations using the Vosko–Wilk–Nusair (VWN) functional<sup>31</sup> to obtain the local potential. Gradient correlations for the exchange (Becke functional)<sup>32</sup> and correlation (Perdew functional)<sup>33</sup> energy terms were included self-consistently. The program represents molecular orbitals as linear combinations of Slater-type atomic orbitals. All results presented here are based on frozen core spin-unrestricted calculations utilizing double- $\zeta$  basis sets. For carbon and oxygen, a frozen core potential is used for the 1s electrons. The silver frozen core extends to the 3d electrons. Infrared spectra were calculated by carrying out two-point frequency calculations using an integration accuracy of  $10^{-6}$ . The resulting frequencies are reported as calculated, without scaling. As in our previous comparisons of experimental and theoretical vibrational spectra for smaller oxametallacycles,<sup>16,18–20</sup> the silver surface was represented by discrete clusters. Periodic slab calculations for large adsorbates would require the use of very large unit cells and were not attempted in the present work.

## Results

The results are organized in three sections. The first section describes temperature-programmed desorption of styrene oxide on Ag(111). The HREELS results are reported in the second section, while DFT calculations are presented in the final section.

**Temperature-Programmed Desorption.** TPD experiments monitored 20 representative masses which provided a high level of confidence when making the product assignment. This assignment was based on the fragmentation patterns of likely products: styrene oxide, phenylacetaldehyde, and acetophenone. The fragments of these products, even though very similar, contain certain differences that permit us to distinguish one from another. For example,  $m/q = 105$  is the largest fragment in the acetophenone fragmentation pattern, while it is observed only in small amounts in styrene oxide and phenylacetaldehyde. Similarly, the  $m/q = 119$  fragment is present in the styrene oxide cracking pattern while it is not seen in acetophenone and phenylacetaldehyde. Also,  $m/q = 89$  and  $m/q = 90$  fragments are much larger for styrene oxide compared to acetophenone

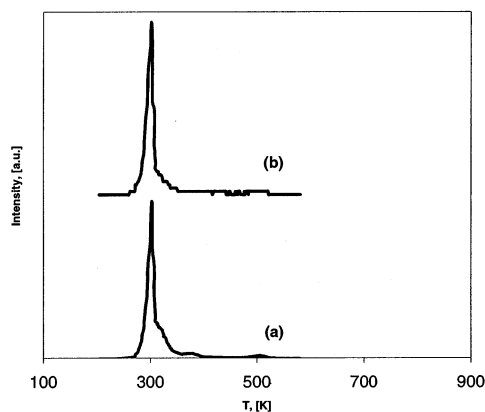


**Figure 1.** TPD spectra for mass fragments (a)  $m/q = 91$  and (b)  $m/q = 119$  following styrene oxide adsorption on the Ag(111) surface at 100 K.

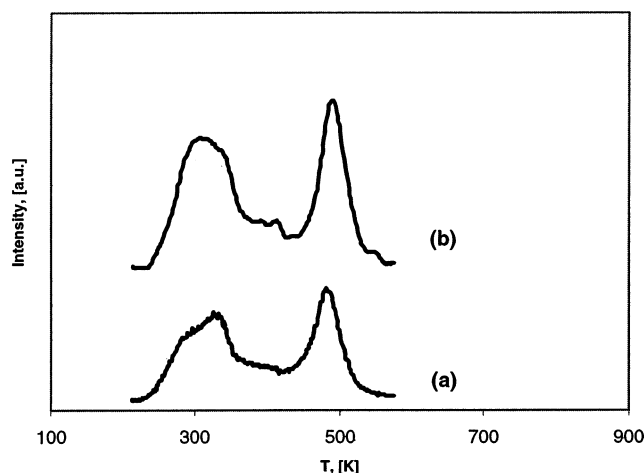


**Figure 2.** TPD spectra for mass fragments (a)  $m/q = 91$  and (b)  $m/q = 119$  following styrene oxide adsorption on the Ag(111) surface at 240 K.

and phenylacetaldehyde. The fragment  $m/q = 91$  is the largest fragment for styrene oxide and phenylacetaldehyde, while  $m/q = 65$  and  $m/q = 92$  appear in both cracking patterns in comparable amounts.

Styrene oxide adsorbed onto the clean Ag(111) surface at 170 K desorbs molecularly at 300 K. In Figure 1, we show the mass fragments  $m/q = 119$ , used to track styrene oxide, and  $m/q = 91$ , the most abundant fragment in the fragmentation patterns of both styrene oxide and phenylacetaldehyde. A careful examination of Figure 1 suggests that the shapes of the peaks for the  $m/q = 91$  and  $m/q = 119$  signals are slightly different. The reason for this is that there is a phenylacetaldehyde impurity that is dosed along with styrene oxide, and which desorbs at a slightly higher temperature than styrene oxide. This results in a small shoulder on the high-temperature side of the principal peak at 300 K in the  $m/q = 91$  spectrum. The 300 K peak saturates at larger exposures and is thus attributed to molecularly adsorbed styrene oxide. There is also a small feature in the TPD spectrum at 485 K; however, the intensity of this peak is too small to permit the identification of the desorbing products.

Figure 2 shows the TPD spectra collected after styrene oxide was adsorbed onto Ag(111) at 245 K. Again, we observe desorption of molecularly adsorbed styrene oxide at 300 K, but there is also a sizable peak at around 485 K. This peak is attributed to styrene oxide plus phenylacetaldehyde. The detection of only a very small signal for the  $m/q = 105$  mass fragment leads us to conclude that acetophenone is not one of the

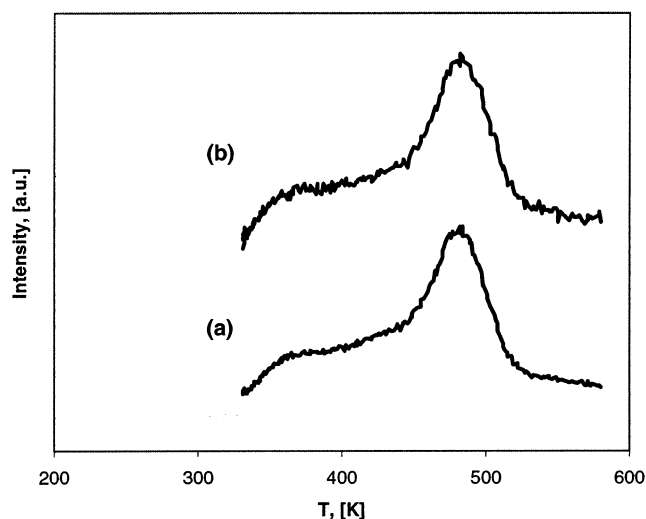


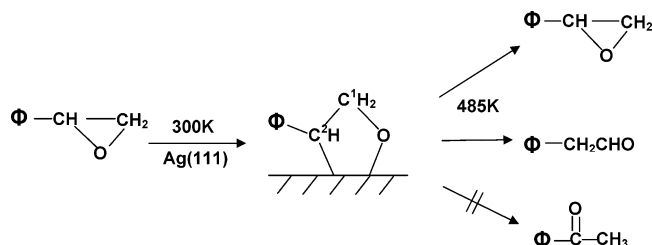
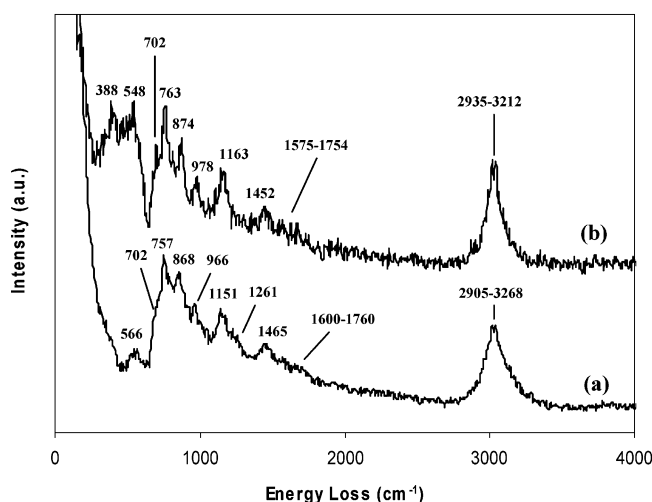
**Figure 3.** TPD spectra for mass fragments (a)  $m/q = 91$  and (b)  $m/q = 119$  following styrene oxide adsorption on the Ag(111) surface at 320 K.

products. Figure 3 shows the TPD spectrum collected after styrene oxide has been adsorbed on Ag(111) at 320 K. Here, we only detect a high-temperature peak which is again assigned to a combination of styrene oxide and phenylacetaldehyde. The high temperature,  $\sim 485$  K, at which these products desorb indicates that a strongly bound intermediate is formed by styrene oxide adsorption on Ag(111) above  $\sim 200$  K. As stated above, molecular styrene oxide desorbs from Ag(111) at  $\sim 300$  K. Moreover, it is highly unlikely that any adsorbed molecule would remain at temperatures as high as 485 K. Examination of figures 1–3 suggests that there is an activation energy associated with the formation of this intermediate, as evidenced by the fact that no appreciable desorption at 485 K is detected after dosing styrene oxide onto Ag(111) at 100–200 K. The activation energy requirement implies that bond breaking within the original molecule must take place. This bond breaking must be accompanied by the formation of bonds to the surface to create a stable surface intermediate. Activated opening of the epoxide ring to form an oxametallacycle has previously been observed for epoxybutene on Ag(110) and for ethylene oxide on Ag(111). The product distribution associated with the 485 K desorption peak implies that the C–C bonds of styrene oxide remain intact, as no lower molecular weight products are observed. The same is true for the C–H bonds as evidenced by the lack of dehydrogenated products. The only remaining possibility is that a C–O bond on one side of the epoxide ring is broken. Cleavage of a single C–O bond would result in the formation of a surface oxametallacycle, which could subsequently react to form products which maintain the molecular weight of styrene oxide, as previously shown for the analogous reactions of ethylene oxide<sup>19</sup> and epoxybutene.<sup>20</sup> The lack of acetophenone in the product distribution implies that the bond that is cleaved in the activated adsorption of styrene oxide onto Ag(111) is the one that links oxygen to the carbon that is bonded to the benzene ring. The C–O bond that links the terminal carbon to oxygen in the epoxide ring remains intact. Even though the TPD results provide sound evidence that the strongly bound intermediate that thermally decomposes at 485 K on Ag(111) to form styrene oxide and phenylacetaldehyde is an oxametallacycle, a full determination of the nature of this strongly bound intermediate necessitates the use of surface spectroscopic techniques. The results of HREELS experiments are displayed below.

**TABLE 1: Selectivity to Styrene Oxide as a Function of the Amount of the Strongly Bound Surface Intermediate Desorbing at  $T = 485\text{ K}$ <sup>a</sup>**

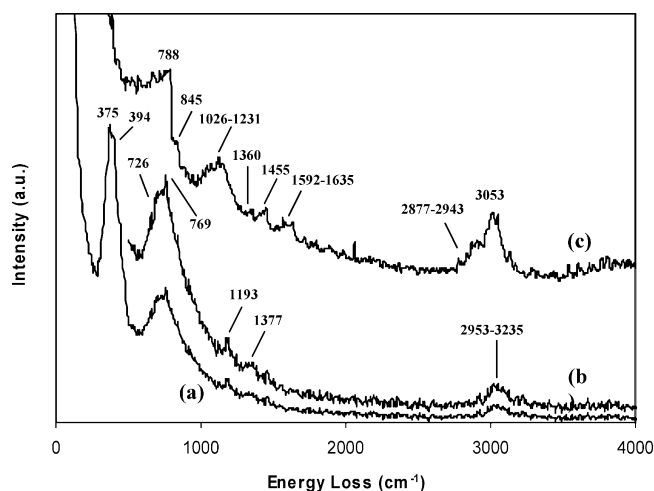
relative coverage	1.00	0.75	0.50	0.45
selectivity	0.70	0.79	0.86	0.92

<sup>a</sup> The amount of the strongly bound surface intermediate is calculated as a ratio of an amount of desorbed product to the amount of product desorbed at maximum coverage.

**Figure 4.** Reaction scheme for styrene oxide on Ag(111) proposed on the basis of TPD experiments.**Figure 5.** HREEL spectra following (a) multilayer and (b) monolayer adsorption on Ag(111) at 100 and 220 K, respectively.

Increasing styrene oxide exposure at elevated temperature,  $>300\text{ K}$ , prior to TPD resulted in an increase in the amount of styrene oxide and phenylacetaldehyde desorbed at high temperature until the desorption peak became saturated at a coverage similar to the saturation coverage of molecularly adsorbed styrene oxide. In Table 1, we show the selectivity of the 485 K reaction channel toward styrene oxide. It can be concluded that the selectivity to styrene oxide decreases slightly as the coverage of the strongly bound surface oxametallacycle intermediate increases. Figure 4 illustrates the basic scheme for the reaction of styrene oxide on Ag(111).

**High-Resolution Electron Energy Loss Spectroscopy.** To identify the surface intermediate involved in the reaction of styrene oxide on the Ag(111) surface, a series of HREELS experiments was conducted. Styrene oxide was first adsorbed on the surface at 110 K and maintained at this temperature for analysis. The resultant spectrum is shown in Figure 5a. On the basis of comparison with reported liquid-phase IR spectra, the spectrum is attributed to multilayers of styrene oxide. A spectrum collected after dosing at 220 K is shown in Figure 5b. As shown by our TPD experiments, this dosing temperature is sufficient to prevent the formation of multilayers; therefore, this observation and the small differences relative to the multilayer spectrum suggest that this spectrum is attributable to monolayer styrene oxide. The vibrational frequencies for this spectrum and the multilayer spectrum are listed in Table 2 along

**Figure 6.** HREEL spectra for the oxametallacycle formed by ring-opening styrene oxide on Ag(111) at 300 K. (a) Spectrum collected for specular scattering. (b) Spectrum in Figure 6a  $\times 2$ . (c) Off-specular spectrum.**TABLE 2: Vibrational Frequencies ( $\text{cm}^{-1}$ ) of 110 K, 220 K HREELS Spectra, and DFT-Predicted Frequencies of Molecular Styrene Oxide**

DFT-predicted, styrene oxide	HREELS, 110 K dose	HREELS, 220 K dose
386		388
527, 578	566	548
703, 707	702	702
754, 771	757	763
800	868	874
919	923	
979	966	978
1120	1083	
1179	1151	1163
1361		
1452, 1494	1465	1452
1588	1600–1760	1575–1754
3032, 3124, 3146	2905–3268	2935–3212

with the vibrational frequencies of gaseous styrene oxide calculated using DFT. The DFT results are discussed in subsequent sections.

Styrene oxide was dosed onto the Ag(111) crystal surface at 300 K in a separate experiment. After pumping the excess styrene oxide from the chamber, the surface was scanned in the specular orientation at room temperature. The resultant spectrum is shown in Figure 6a. The spectrum is significantly different from the spectra assigned to monolayer and multilayer styrene oxide. Consequently, it must represent a species which is chemically different from styrene oxide. This is in accord with our TPD experiments indicating that monolayer and multilayer styrene oxide desorb at or below 300 K. This species reacted at 485 K to reform styrene oxide and a few other products. Because of the difficulty in resolving low intensity losses in the region of 1100–1400  $\text{cm}^{-1}$  shown in the amplified specular scan, Figure 6b, an off-specular scan, shown in Figure 6c, was performed. Analysis of the specular and off-specular HREELS results and comparison to calculated DFT spectra of oxametallacycle intermediates suggest that the species isolated after dosing at 300 K is a surface oxametallacycle as discussed below.

**Density Functional Theory Calculations.** This work continues our use of DFT calculations as a first-principles quantum chemical tool in concert with HREELS and TPD experiments to identify important surface intermediates. Oxametallacycles have been proposed as surface intermediates in numerous



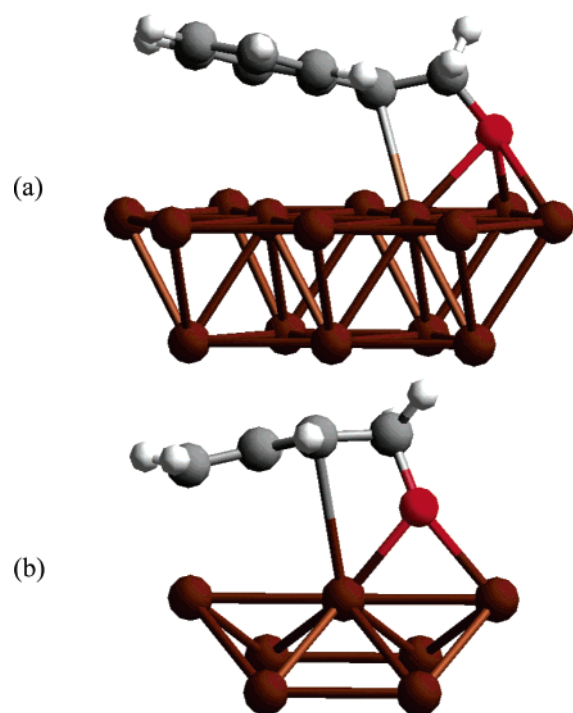


**Figure 7.** Comparison of the DFT-calculated structures of oxametallacycles derived from (a) styrene oxide on Ag(111) and (b) epoxybutene on Ag(110).

reactions, but they have been spectroscopically identified on only a few occasions.<sup>16–20</sup>

The structures for styrene oxide-derived oxametallacycles interacting with one to three surface atoms were calculated on Ag<sub>10</sub> and Ag<sub>15</sub> clusters. From these calculations, it was determined that a structure with oxygen occupying a threefold hollow site, with the C<sup>2</sup> carbon bound to one of the silver atoms of this site, was favored (see Figure 7). In this geometry, previously referred to as an OME structure<sup>34</sup> as the terminal C and O functions of the oxametallacycle interact with a common surface metal atom, the phenyl group is oriented nearly parallel to the crystal surface. Figure 7 compares the most stable oxametallacycles obtained for ring-opening styrene oxide on Ag(111) and epoxybutene on Ag(110).<sup>20</sup> The structural similarities are readily apparent. Frequency calculations were performed for the oxametallacycle on 10- and 15-atom clusters; however, few differences in the calculated spectra were observed, which is consistent with our previous results for EpB-derived oxametallacycles.<sup>20</sup> In Table 3, we report the major frequencies of the computed IR spectra for the OME structure on the Ag<sub>10</sub> and Ag<sub>15</sub> clusters. A comparison of the predicted spectrum for the Ag<sub>15</sub> calculation and the off-specular HREELS scan is shown in Figure 8. It is important to note several items about these spectra. While HREELS and IR have the same dipole selection rules, the calculated IR spectra do not take into account surface selection rules. In particular, the screening of dipole-active modes parallel to the surface is not accounted for in the calculated spectra. Thus, while it is not unreasonable to compare the intensities of the experimental HREEL and theoretical IR spectra, it is necessary to obtain HREEL spectra in an off-specular mode to enhance impact scattering from parallel modes to facilitate comparisons for intermediates that are bonded parallel to the surface, as in the present case.

#### Comparison of Theoretical and Experimental Results.

Upon inspection of the HREEL spectrum following styrene oxide adsorption at 300 K, it is apparent that the relative peak

intensities above 1000 cm<sup>-1</sup> are quite low. Energy losses in this region (1000–1600 cm<sup>-1</sup>) are predominantly attributable to the phenyl ring vibrations and CH modes. The attenuation of these vibrations suggests that phenyl group modes are diminished as a consequence of the surface dipole selection rule, since TPD experiments show that the phenyl ring remains intact in all products. Thus, the phenyl ring must be oriented virtually parallel to the crystal surface. Our DFT-derived optimized geometry for the intermediate on the 10- and 15-atom silver clusters confirms this interpretation. However, this also makes it difficult to make detailed comparisons of the measured and calculated spectra, because the intensity of the former is so low in this frequency region. The presence of various small peaks above 1000 cm<sup>-1</sup> does suggest a more complex structure that can be probed by enhancing impact scattering. By increasing the beam energy and performing off-specular data collection, further details were elucidated in the region above 1000 cm<sup>-1</sup> for comparison with the DFT-predicted IR spectrum of the oxametallacycle. In the specular HREEL spectrum, strong features are observable at 375 and 394 cm<sup>-1</sup>. DFT calculations predict strong vibrational modes at approximately 300 and 480 cm<sup>-1</sup> which correspond to carbon–oxygen–silver stretching and a symmetric deformation of the phenyl ring, respectively. We believe that the differences are largely explicable by the approximation of the Ag(111) crystal surface as a 10- or 15-atom cluster. Vibrational modes at these low frequencies involve some motion of the silver atoms. Considering the 15-atom structure shown in Figure 7, the oxygen atom is bonded to silver atoms at the edge of the cluster. Vibrations involving these atoms are likely to be less accurately represented. Expansion of the cluster to mitigate such edge effects might improve the agreement somewhat, but at significantly greater computational cost.

The second major feature in the specular HREEL spectrum is comprised of two features at 726 and 769 cm<sup>-1</sup>. DFT calculations for the 15-atom cluster geometry produce CH out-of-plane wagging modes at frequencies of 735 and 795 cm<sup>-1</sup>. These frequencies are good matches for the experimental spectrum and represent modes with notable dipole moments normal to the surface. Consequently, such modes are prominent in the HREEL spectrum.

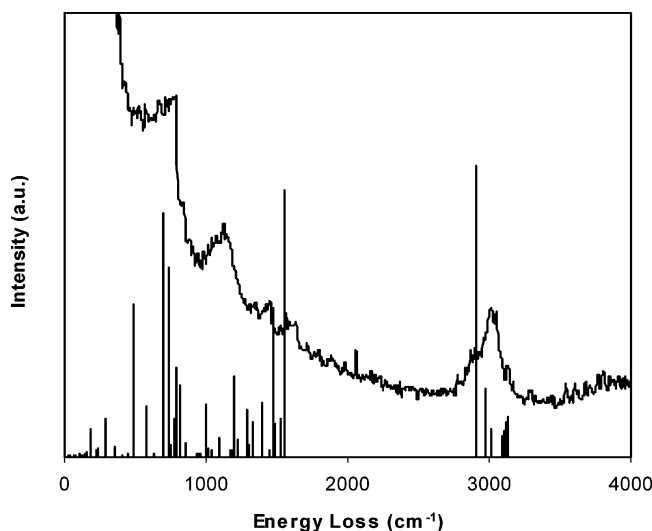
Minor features appear in the specular spectrum at 1193, 1360–1390, and 2953–3235 cm<sup>-1</sup>. The minimal intensities of these features suggest that they correspond to phenyl group motion and CH modes parallel to the surface, that is, in the plane of the molecule. The enhancement of these features in the off-specular spectrum confirms this conclusion and demonstrates that these modes may be made visible by impact scattering. Our DFT calculations assign the 1197 cm<sup>-1</sup> peak to phenyl hydrogen in-plane wagging modes, the 1390 cm<sup>-1</sup> peak to CH wagging and phenyl ring breathing, the 1555 cm<sup>-1</sup> mode to phenyl ring breathing, and the 2900–3130 cm<sup>-1</sup> features to a series of phenyl ring hydrogen stretches. These calculated vibrational modes correspond fairly well to the experimental results in Figure 8. The off-specular spectrum reveals additional vibrational modes at 1455, 1559–1635, and 2877–2943 cm<sup>-1</sup>. DFT predicts that additional vibrations associated with the C<sup>1</sup>–H symmetric stretch should appear at 1472 cm<sup>-1</sup>, and phenyl ring breathing and CH stretches at 1555 and 2908 cm<sup>-1</sup>, respectively.

#### Discussion

The oxametallacycle formed by ring-opening styrene oxide on Ag(111) fits well within the family of such intermediates previously examined with experimental and theoretical tools on

**TABLE 3: Major Vibrational Frequencies ( $\text{cm}^{-1}$ ) of 300 K Intermediate**

normal mode	HREELS, intermediate on Ag(111) specular	HREELS, intermediate on Ag(111) off-specular	DFT-predicted, OME frequencies Ag <sub>10</sub>	DFT-predicted OME frequencies Ag <sub>15</sub>
C—O—M	375, 394		304	284
symmetric phenyl deform. (boat)			478	489
phenyl ring bending			670	693
phenyl C—H wag out of plane (chair)	726		734	735
C <sup>2</sup> —H wag	769	788	776	795
O—C—C symmetric stretch			818	818
C <sup>2</sup> H-wag, phenyl ring bend		845	839	856
C <sup>1</sup> rock			919	994
in-plane phenyl H-wag, C <sup>1</sup> —C <sup>2</sup> stretch	1193	1026–1231	1178, 1191	1197
C—H wag, phenyl breathing	1360–1390	1380	1293, 1394	1289, 1390
C <sup>1</sup> —H sym stretch		1455	1461	1472
C <sup>1</sup> —H asym stretch, C <sup>2</sup> —H stretch			1491	1522
phenyl ring breathing		1559–1635	1539	1555
phenyl ring CH stretches		2877–2943	2892	2908
phenyl ring CH stretches			2976	2969
phenyl ring CH stretches	2953–3235	3053	3090	3132

**Figure 8.** Comparison of the off-specular, experimental HREEL spectrum from Figure 6c with the calculated IR spectrum for the styrene oxide oxametallacycle structure in Figure 7a.

silver surfaces. As shown in Figure 7, the structure is analogous to that obtained for the EpB-derived oxametallacycle. In all cases of epoxide ring opening on silver surfaces observed to date, the ring-opening reaction was an activated process, requiring surface temperatures above 200 K. The principal reaction product in each case is the parent epoxide, accompanied by small amounts of products with the same number of carbon atoms.

More importantly, the characteristics of the styrene oxide-derived oxametallacycle confirm several previous extrapolations based on experiments and calculations for epoxybutene. We have previously reported that DFT calculations for simple oxametallacycles incorporating even one silver atom suggest that the thermodynamically preferred structure is one in which the silver atom is inserted into the C<sup>2</sup>—O bond of the epoxide to form a linear isomer, *provided that the substituent group is unsaturated*.<sup>35</sup> Thus, the oxametallacycles which would be formed from epoxybutene, isoprene oxide, and styrene oxide were predicted to have the hydrocarbon ligands pendant from C<sup>2</sup> (see Figure 4 for the numbering scheme), rather than C<sup>1</sup> (which would result in a branched isomer).<sup>33</sup> This prediction was confirmed by experiment for EpB on Ag(110)<sup>20</sup> and now for styrene oxide on Ag(111). Both the HREELS results showing that the phenyl ring is nearly parallel to the surface for the StO-derived oxametallacycle and the TPD results that show formation of phenylacetaldehyde but not acetophenone support the oxametallacycle structure depicted in Figure 7 and not the

branched isomer. Interestingly, our earlier DFT calculations<sup>35</sup> suggested that the oxametallacycles formed from mono-olefin epoxides, for example, propylene and butylene oxides, should be branched rather than linear. To date, however, successful ring opening of mono-olefin epoxides to form such species has not been accomplished.

Like the only other oxametallacycle derived from the epoxide of a conjugated olefin (EpB), the oxametallacycle formed by ring-opening styrene oxide exhibits much greater thermal stability than the corresponding species derived from ethylene oxide. The oxametallacycles of EpB and StO undergo ring closure at ca. 485 K, in contrast to that from ethylene oxide, which reacts just above 300 K. Thus, the presence of pendant vinyl or phenyl groups clearly stabilizes oxametallacycles on silver. The peak temperatures for ring closure of styrene oxide- and epoxybutene-derived oxametallacycles correspond to activation energies of 31–32 kcal/mol, if one assumes a normal preexponential factor of  $10^{13} \text{ s}^{-1}$ . However, both the HREELS and DFT results show little evidence for perturbation of the phenyl group of the StO-derived oxametallacycle by the surface. While interactions of this group with the surface may contribute to oxametallacycle stability, they do not produce detectable deformation or rehybridization.

Finally, we compare the present results with the previous TPD data of Hawker et al.<sup>7</sup> for the production of styrene oxide from coadsorbed styrene and oxygen atoms on Ag(111). These workers observed the evolution of an epoxide product at ca. 500–510 K in their experiments. This temperature is in excellent agreement with the peak temperature observed here for ring closure of the StO-derived oxametallacycle. We conclude, therefore, that the rate of styrene oxide formation in their experiments corresponds to the rate of the ring closure of an oxametallacycle intermediate formed at lower temperature by addition of oxygen atoms to adsorbed styrene. In other words, epoxidation of styrene proceeds through an oxametallacycle intermediate, just as for those of ethylene and butadiene on silver surfaces and catalysts. The stability of the StO- and EpB-derived oxametallacycles in particular makes these appealing targets for further spectroscopic studies.

## Conclusions

Styrene oxide undergoes an activated ring opening on Ag(111) to produce a stable oxametallacycle intermediate. HREELS and DFT results demonstrate that the pendant phenyl group in this structure is nearly parallel to the surface. The oxametallacycle reacts at 485 K to reform the parent styrene

oxide, plus small amounts of phenylacetaldehyde. The correspondence of these observations with those previously reported for styrene oxidation on this surface indicates that styrene epoxidation occurs via a surface oxametallacycle intermediate on silver.

**Acknowledgment.** We gratefully acknowledge the support of the U.S. Department of Energy, Office of Science, Division of Chemical Sciences (Grant FG02-84ER 13290) for research at the University of Delaware, as well as support for DFT calculations at Pacific Northwest National Laboratory through computational grand challenge project 3568. K.U. was supported by the NSF REU summer program. We also thank Barr Halevi and Gordon Wang for assistance with HREELS measurements.

## References and Notes

- (1) *Chem. Eng. News* **1999**, 77, 33.
- (2) van Santen, R. A.; Kuipers, H. P. C. *Adv. Catal.* **1987**, 35, 265.
- (3) Serafin, J. G.; Liu, A. C.; Seyedmonir, S. R. *J. Mol. Catal.* **1998**, 131, 157.
- (4) Monnier, J. R. *Stud. Surf. Sci. Catal.* **1997**, 110, 135.
- (5) Monnier, J. R.; Muehlbauer, P. J.; U.S. Patent 5 138 077, 1992; to Eastman Chemical Company.
- (6) Monnier, J. R.; Muehlbauer, P. J.; U.S. Patent 4 950 773, 1990; to Eastman Chemical Company.
- (7) Hawker, S.; Mukoid, C.; Badyal, J. P. S.; Lambert, R. M. *Surf. Sci.* **1989**, 219, L615.
- (8) Grant, R. B.; Lambert, R. M. *J. Catal.* **1985**, 92, 364.
- (9) Roberts, J. T.; Madix, R. J. *J. Am. Chem. Soc.* **1988**, 110, 8540.
- (10) Mukoid, C.; Hawker, S.; Badyal, J. P. S.; Lambert, R. M. *Catal. Lett.* **1990**, 4, 57.
- (11) Linic, S.; Barteau, M. A. *J. Catal.* **2003**, 214, 200.
- (12) Monnier, J. R.; Medlin, J. W.; Barteau, M. A. *J. Catal.* **2001**, 203, 362.
- (13) Bocquet, M. L.; Michaelides, A.; Loffreda, D.; Sautet, P.; Alavi, A.; King, D. A. *J. Am. Chem. Soc.* **2003**, 125, 5620.
- (14) Stegelmann, C.; Schiodt, N. C.; Campbell, C. T.; Stoltze, P. *J. Catal.* **2004**, 221, 630.
- (15) Linic, S.; Barteau, M. A. *J. Am. Chem. Soc.* **2003**, 125, 4034.
- (16) Jones, G. S.; Mavrikakis, M.; Barteau, M. A.; Vohs, J. M. *J. Am. Chem. Soc.* **1998**, 120, 3196.
- (17) Wu, G.; Stacchiola, D.; Kaltchev, M.; Tysoc, W. T. *Surf. Sci.* **2000**, 463, 81.
- (18) Linic, S.; Medlin, J. W.; Barteau, M. A. *Langmuir* **2002**, 18, 5197.
- (19) Linic, S.; Barteau, M. A. *J. Am. Chem. Soc.* **2002**, 124, 310.
- (20) Medlin, J. W.; Barteau, M. A.; Vohs, J. M. *J. Mol. Catal. A* **2000**, 163, 129.
- (21) Force, E. L.; Bell, A. T. *J. Catal.* **1975**, 38, 440.
- (22) Cant, N. W.; Hall, W. K. *J. Catal.* **1978**, 52, 81.
- (23) Campbell, C. T. *J. Catal.* **1985**, 94, 436.
- (24) Linic, S.; Jankowiak, J.; Barteau, M. A. *J. Catal.* **2004**, 224, 489.
- (25) Davis, J. L.; Barteau, M. A. *Surf. Sci.* **1989**, 208, 383.
- (26) Jones, G. S.; Barteau, M. A. *J. Vac. Sci. Technol., A* **1997**, 15, 1667.
- (27) Plank, R. V.; Vohs, J. M. *Surf. Sci.* **1995**, 340, L971.
- (28) Baerends, E. J. *ADF version 1999.02*.
- (29) Baerends, E. J.; Elis, D. E.; Ros, P. *Chem. Phys.* **1973**, 2, 41.
- (30) Baerends, E. J.; Ros, P. *Quantum Chem. Symp.* **1978**, 12, 169.
- (31) Vosko, S. H.; Wilk, L.; Nusair, M. *Can. J. Phys.* **1980**, 58, 1200.
- (32) Becke, A. D. *Phys. Rev. A* **1988**, 38, 3098.
- (33) Perdew, J. P. *Phys. Rev. B* **1986**, 33, 8822.
- (34) Mavrikakis, M.; Doren, D. J.; Barteau, M. A. *J. Phys. Chem. B* **1998**, 102, 394.
- (35) Medlin, J. W.; Barteau, M. A. *J. Phys. Chem. B* **2001**, 105, 10054.